Electronic Supplementary Material (ESI) for Journal of Materials Chemistry C.

Supporting Information

Natural bioproducts hybridization creates transient dynamic electret nanogenerators

Liang Lu [a, b, c, ⊥], Chuanfeng Wang [a, b, c, ⊥], Zhu Liu [a, b, c], Yu Lai [a, b, c], Wei Li [a], Dingyun Shao [a], Jun Lu [a, b, #, *], Weiqing Yang [a, c, *]

[a] Key Laboratory of Advanced Technologies of Materials, Ministry of Education, School of Materials Science and Engineering, Southwest Jiaotong University, Chengdu 610031, Sichuan, China

[b] School of Chemistry, Southwest Jiaotong University, Chengdu 610031, Sichuan, China

[c] Research Institute of Frontier Science, Southwest Jiaotong University, Chengdu 610031, Sichuan, China

[⊥] These authors equally contributed to this work.

[#] Other used names Jun Lv and Jun Lyu.

[*] Corresponding authors. E-mail: junluprc@hotmail.com (J. Lu), wqyang@swjtu.edu.cn (W.Q. Yang).

Experimental Section

Materials and Reagents

Polyhydroxybutyrate (PHB) was provided by TianAn Biologic Materials Co., Ltd, Ningbo, China (M_n: ~85000; M_w: ~240000). Sulfonated cellulose nanocrystals (S-CNCs) were supplied by Qihong Technology Co., Ltd, Guilin, China. The needle-like S-CNCs, with a diameter of 5-10 nm and a length of 100-500 nm, were produced by sulfuric acid hydrolysis of natural plant cellulose. Chloroform and N, N-dimethylformamide (DMF) were of analytical grade, and were purchased from Kelong Chemical Co., Ltd, Chengdu, China. They were used as received.

Electrospinning of S-CNCs/PHB Hybrid Nanofibers

A schematic diagram of the manufacturing process of electrospun S-CNCs/PHB nanofibers is shown in Fig. S1a, Supporting Information. First, the S-CNCs in the original aqueous solution were dispersed in DMF solvent using a rotary evaporator machine at 50 °C for 1.5 h. After the solvent exchange, the S-CNCs in DMF were further dispersed by ultrasonic treatment to give a uniform, transparent S-CNCs/DMF dispersion. Then 0.9 g of PHB was added into 9 ml of chloroform and stirred in a sealed environment in a water bath at 60℃ for 3 h to obtain a homogeneous solution of PHB/chloroform. After that, 1ml of the S-CNCs/DMF dispersion, with different S-CNCs contents, was added to the above PHB/chloroform solution. The mixture was further agitated in a water bath and then sonicated to give a uniform spinning solution.

The as prepared spinning solution was injected into a 10 mL syringe, connected to a blunt-end needle with an inner diameter of 0.41 mm. Using a direct current (DC) spinning setup, the electrospinning was carried out at an applied voltage of 11 kV. The receiving distance was set to 20 cm, and the flow rate was maintained at 10 μL min^{-1}. A grounded, high-speed roller was used as the collector. The rotational speed was held constant at 4000 rpm. After electrospinning, the electrospun thin films consisting of highly oriented nanofibers were removed from the roller and subsequently cut into samples of useful size. The electrospun S-CNCs/PHB nanofibers with different S-CNCs contents are denoted here as S-CNCs-x. The x represents the mass ratio of S-CNCs to PHB, namely x per hundred. For

S-CNCs-0, S-CNCs-1, and S-CNCs-3 nanofibers, the mass ratios of S-CNCs to PHB are 0, 0.01, and 0.03, respectively.

Characterization of Materials

Transmission electron microscopy (TEM) was performed using a JEOL JEM-2100F instrument. Scanning electron microscopy (SEM) was conducted on a JSM-6330F apparatus. Energy dispersive spectroscopy (EDS) was carried out using an Oxford X-Max 80 spectrometer. Attenuated total reflectance Fourier transform infrared (ATR-FTIR) spectra were obtained using a Nicolet iS20 spectrometer. Differential scanning calorimetry (DSC) measurements were made at atmospheric pressure using a TA-Q20 calorimeter. The crystallinity (X_c) of the hybrid samples was calculated using the following equation [1]:

$$X_c = \frac{\Delta H_m}{\Delta H_m^0 \times \omega(PHB)} \times 100\% \quad (1)$$

where ΔH_m is the melting enthalpy of a hybrid sample, and *ω(PHB)* is the mass ratio of PHB in a hybrid sample. ΔH_m^o is the equilibrium melting enthalpy of PHB crystal. It was assumed to be 146 J/g according to Barham et al [2, 3].

X-ray diffraction (XRD) patterns were collected on a PANalytical X'pert PRO diffractometer. X-ray pole figures were measured using a PANalytical Empyrean Series 2 diffraction system. The polar angle α ranged from 0 to 75°, and the azimuthal angle β ranged from 0 to 360°, with a step size of 5° for both α and β. The measured incomplete pole figures were input into Matlab toolbox MTEX, an opensource package for texture analysis and modeling [4-6]. Then the complete pole figures were recomputed based on orientation distribution function (ODF), and the pole densities at specific locations were obtained from the complete pole figures. The pole density was calculated as described in references [5, 6].

Tensile strength and elongation at break of the S-CNCs-x fiber films (30 mm × 20 mm) were determined at room temperature using a LDW-1 universal testing machine with a crosshead speed of 10 mm/min. In the test, the tensile direction was consistent with the fiber orientation of the electrospun S-CNCs-x fiber films. At least five specimens were measured for each group of samples and the average values were reported.

Degradation of Biohybrid Nanofibers

The hydrolysis of electrospun S-CNCs/PHB nanofibers was tested in the closed tubes containing an aqueous solution of sodium hydroxide. The free-standing S-CNCs/PHB fiber films used were of similar size and similar mass, but varied in S-CNCs content. Each sample was immersed in an alkali aqueous solution at pH 12, and the hydrolytic temperature was kept constant at 37°C. The samples were removed from the aqueous solution at regular intervals. They were washed with distilled water, and then placed in a vacuum oven to evaporate the remaining water. After that, these samples were weighed, and the mass changes were recorded. The residual weight fraction (Φ) of each sample was calculated as follows [7]:

$$\Phi = \frac{W_t}{W_0} \times 100\% \tag{2}$$

where W_0 is the initial mass before hydrolysis, and W_t is the residual mass after hydrolysis.

Fabrication of Biopiezoelectret Nanogenerators

The S-CNCs-x based biopiezoelectret nanogenerator was designed by a specific sandwich structure, as shown in detail in Fig. S1b, Supporting Information. It consisted of S-CNCs/PHB nanofiber film, copper (Cu) electrode, and polyurethane (PU) tape. Two square copper foils, with an edge length of 1.5 cm, were cut and attached to the upper and lower sides of the fibrous film as the electrodes. The thickness of the electrospun film used was 300 μm, and the area was slightly larger than that of the copper electrode to avoid an electrical short-circuit at operation. Then the trilayer square, Cu:S-CNCs/PHB:Cu, was encapsulated using transparent PU tape as a protective layer. Finally, two acrylic sheets were installed on both sides of the biopiezoelectret device. This ensured a smooth impact in the subsequent piezoelectric measurements. The impact head of the measurement system was also made of the same acrylic resin. This ensured eliminating the possible interference of triboelectric charges.

Test of Devices

The piezoelectric properties of S-CNCs-x based biopiezoelectret nanogenerator were evaluated by measuring the electrical outputs under dynamic impulse forces. The home-

made impact measurement system is schematically shown in Fig. 1c, Supporting Information. A linear motor, model NTIAG HS01-37×166, was used as the impulse source. The output voltage signals were measured by a Keithley 6514 system electrometer. The output current signals were measured by a Stanford Research SR570 low-noise current preamplifier. A switching polarity test was also performed for the S-CNCs-x nanogenerator. The direction of the output electrical signals changed when the electrode connection was swapped (Fig. S1d, Supporting Information). This confirmed that the output signals resulted from the direct piezoelectric responses of biopiezoelectret device rather than from the noise of measurement system or environment [8, 9].

Monitoring of Human Physiology

The relevant biological signals were collected from the recruited volunteers. The informed consent was obtained before testing. These experiments involving human subjects were performed in compliance with the local laws and institutional guidelines. All experiments involving human subjects are not subject to the local institutional ethical review committee due to the non-invasive application of the device on human body, according to the Chapter 3, Article 32 of the Regulations on the Ethical Review of Life Science and Medical Research Involving Human Subjects, jointly designed by the National Health Commission of the People's Republic of China, Ministry of Education of the People's Republic of China, Ministry of Science and Technology of the People's Republic of China, and National Administration of Traditional Chinese Medicine.

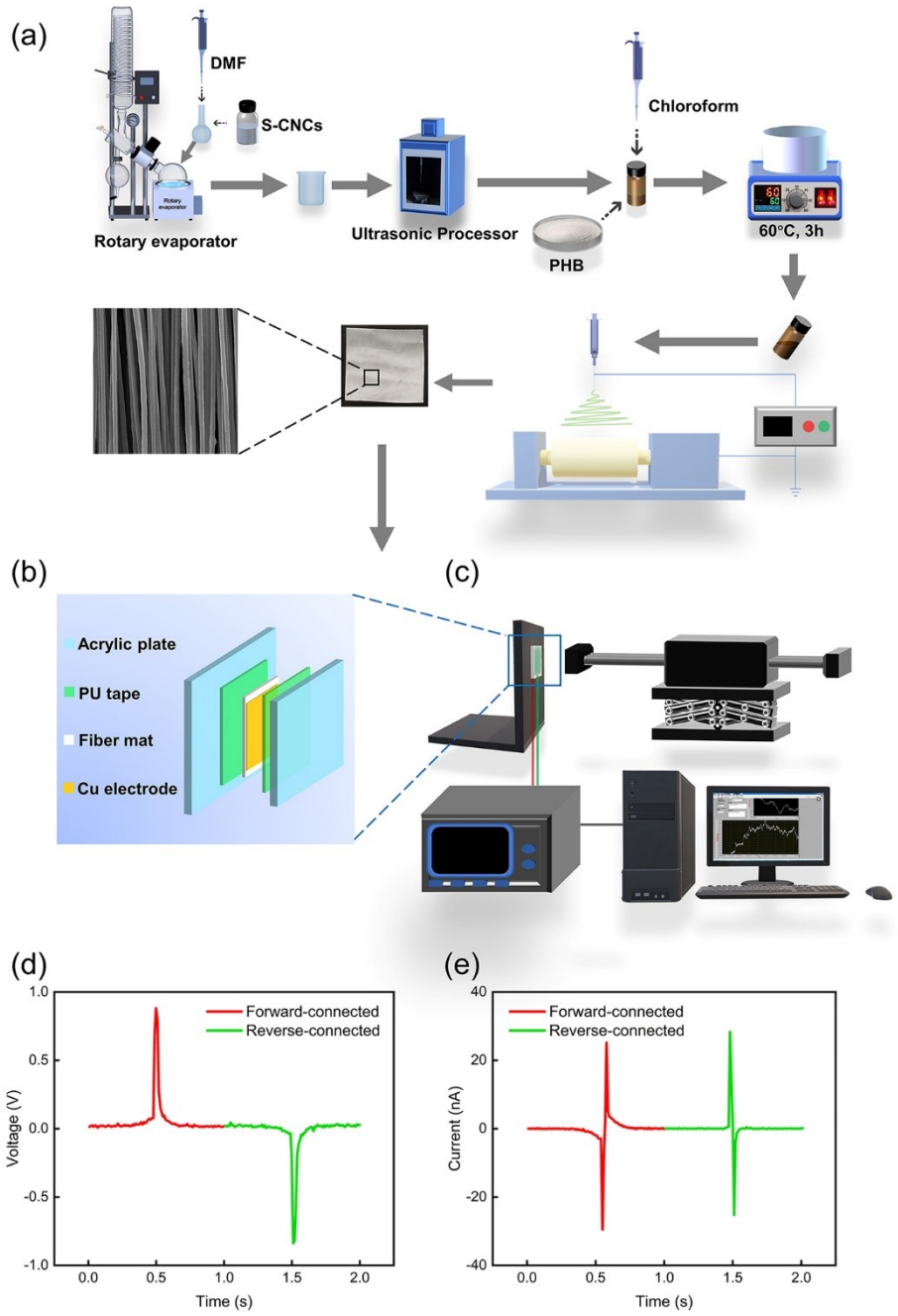

Fig. S1. (a) Schematic illustration of the manufacturing process of electrospun S-CNCs-x nanofibers. The illustration includes a digital image of a free-standing thin film consisting of the uniaxially aligned nanofibers. (b) Schematic diagram illustrating the structural assembly of the tested S-CNCs-x samples. (c) Schematic drawing of the impact measurement system for collecting the generated piezoelectric output. (d) Output voltage signals and (e) output current signals of a S-CNCs-3 nanofiber based biopiezoelectret nanogenerator, in forward connection (left) and reverse connection (right) to the measurement system, respectively.

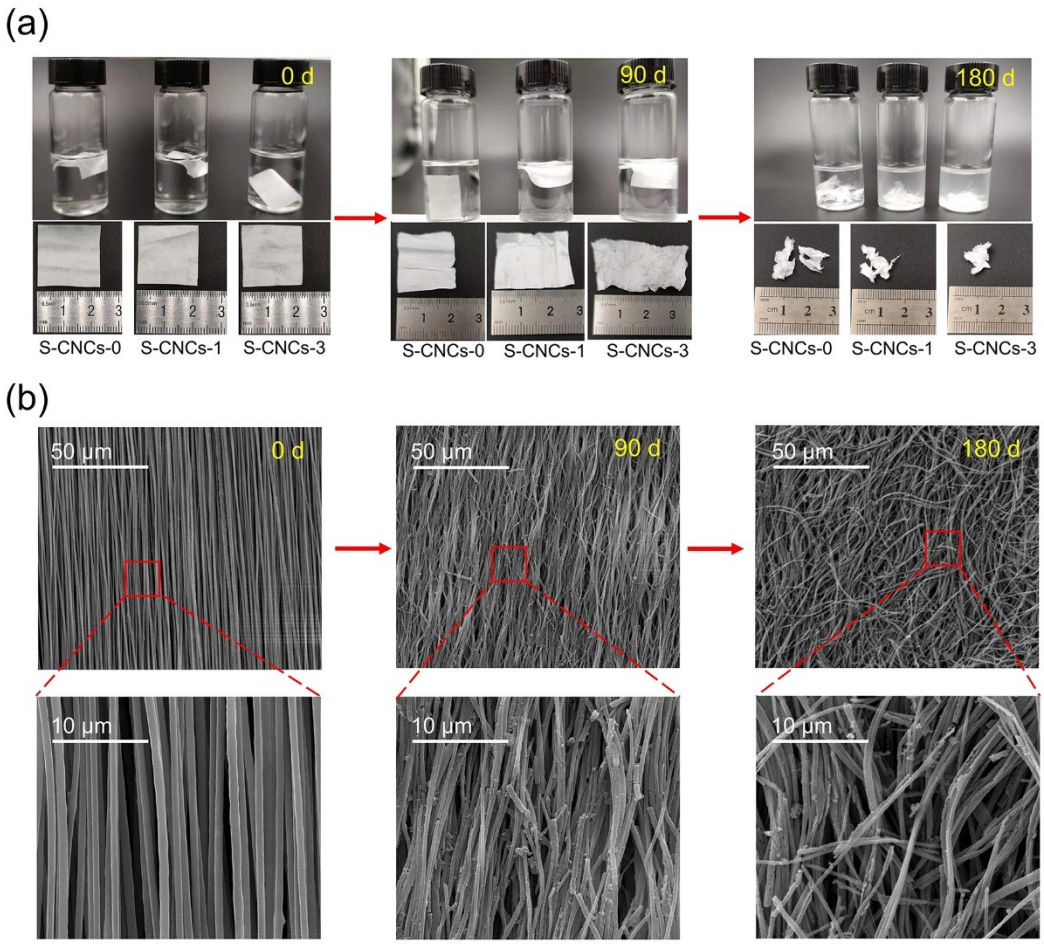

Fig. S2. (a) Digital pictures from left to right showing the S-CNCs-x fiber films being hydrolyzed for 0, 90, and 180 days, respectively. (b) From left to right: SEM images of the S-CNCs-3 fiber film being hydrolyzed for 0, 90, and 180 days, respectively.

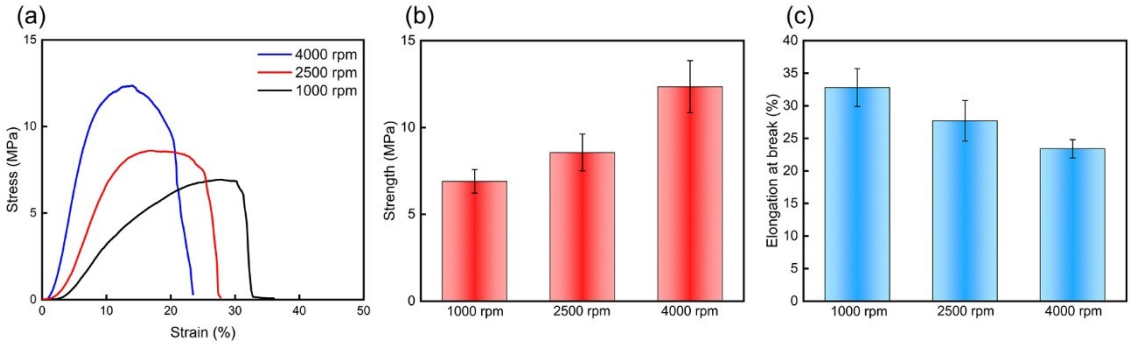

Fig. S3. Mechanical properties of the electrospun S-CNCs-0 fiber films prepared at different rotational speeds of roller collector: (a) stress-strain curves, (b) tensile strength, and (c) elongation at break.

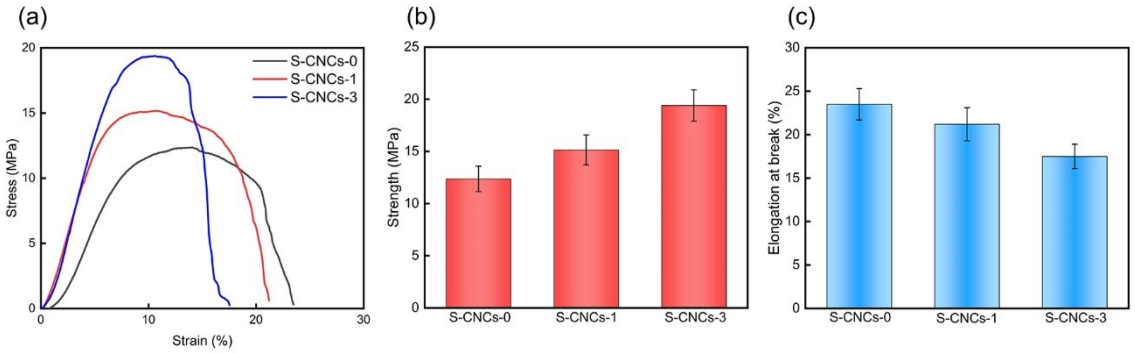

Fig. S4. Mechanical properties of the electrospun S-CNCs-x fiber films with different S-CNCs contents: (a) stress-strain curves, (b) tensile strength, and (c) elongation at break. The rotational speed of roller collector was kept constant at 4000 rpm for the electrospinning of the S-CNCs-x fiber films.

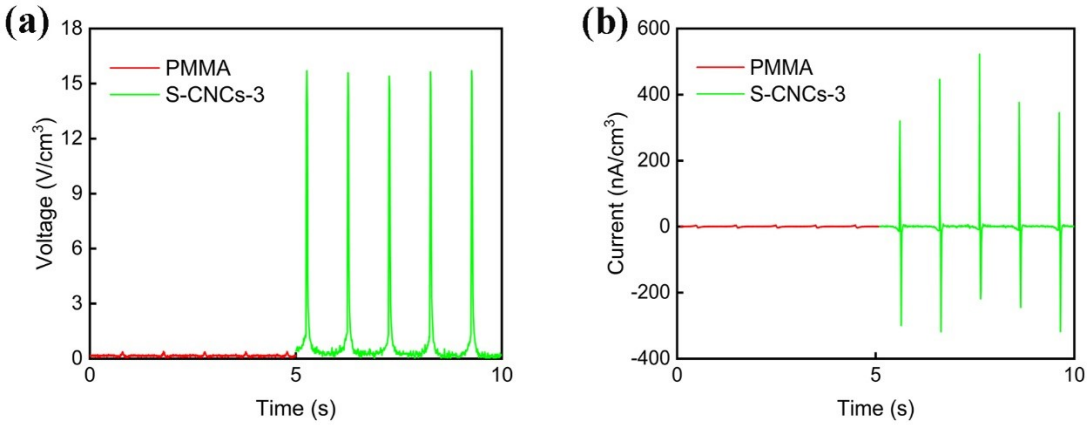

Fig. S5. A comparison of output voltage (a) and output current (b) of the non-piezoelectic polymethyl methacrylate (PMMA) plate based device and the piezoelectric S-CNCs-3 fiber based device, respectively. Both devices belong to the sandwich sructure using copper foil as the electrode material. The Cu:PMMA:Cu trilayer square and the Cu:S-CNCs-3:Cu trilayer square were encapsulated with polyurethane tape for the device-level testing, respectively. The devices were stimulated using a 4-N and 1-Hz impulse force.

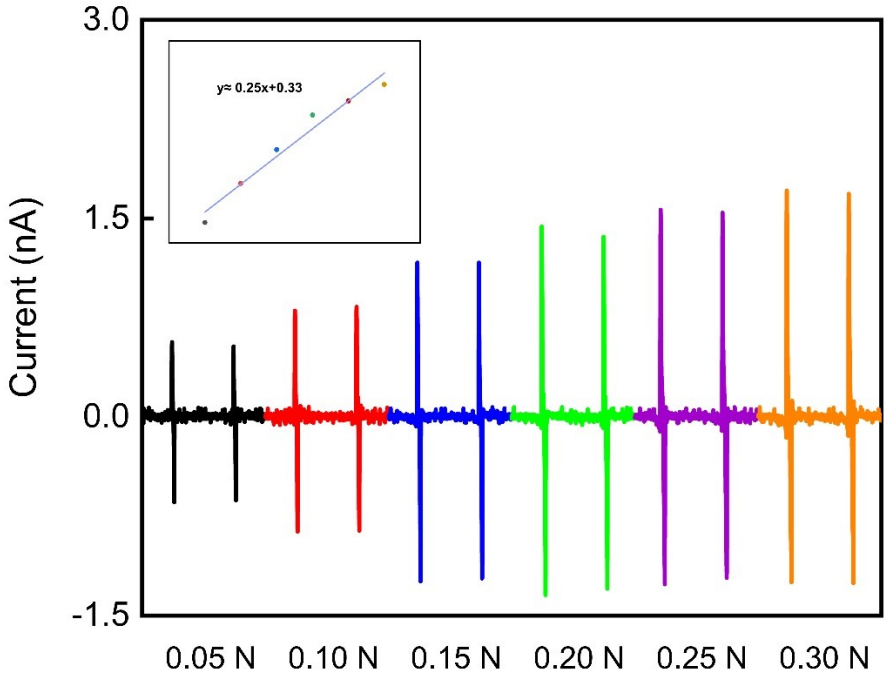

Fig. S6. Output piezoelectric signals of S-CNCs-3 fiber based device under the very small impulse forces and at the frequency of 1.0 Hz. The inset shows the linear sensitivity of output piezoelectric signal in the ultralow-stress regime (0.05-0.30 N).

Table S1. A comparison of the piezoelectric performance of S-CNCs/PHB based device with the previously reported piezoelectric nanogenerators based on degradable, natural bio-origin materials.

No.	Material	Electrode	Treatment	Areal size (mm^2)	Thickness (μm)	Voltage/ Current	Voltage density [a] ($V\ cm^{-3}$)	Current density [a] ($\mu A\ cm^{-3}$)	Sensing application	Ref.
1	Bacteriophage	Au	Unpoled	100	NF	0.4 V/ 6 nA	—	—	NF	[10]
2	Phage nanopillars	Au	Unpoled	NF	NF	0.14 V/ 9.5 nA	—	—	NF	[11]
3	Fish skin collagen	Ag	Unpoled	138	250	2 V/ 20 nA	57.97	0.58	Human physiology monitoring	[12]
4	Prawn shell chitin	Au	Unpoled	12.95 × 7.37	130	1 V/ 1 nA	81	0.081	Human physiology monitoring	[13]
5	Squid pen β-chitin	Ag	Unpoled	60 × 100	35	1.04 V/ 177 nA cm^{-2}	4.95	50.57	Acoustics stimuli detection	[14]
6	Aloe vera extract	Au/Al	Poled	40 × 40	27	1.19 V/ 547 nA	27.55	12.66	Human joint motion sensing	[15]
7	Peptide	Au	Poled	12 × 12	NF	0.6 V/ 7 nA	—	—	NF	[16]
8	ZnO/cellulose	Au	Poled	NF	40	1.5 V/ 80 nA	—	—	Book-page turning motion monitoring	[17]
9	**S-CNCs/PHB**	**Cu**	**Unpoled**	**15 × 15**	**300**	**1.92 V/ 81 nA**	**28.5**	**1.2**	**Human physiology monitoring; acoustics wave pattern identification; smart sports training**	**This work**

[a] Values calculated based on other parameters reported in the references.

References

[1] C. Wang, L. Lu, W. Li, D. Shao, C. Zhang, J. Lu and W. Yang, Green-in-green biohybrids as transient biotriboelectric nanogenerators, *iScience*, 2022, **25**, 105494.

[2] P. J. Barham, A. Keller, E. L. Otun, P. A. Holmes, Crystallization and morphology of a bacterial thermoplastic: poly-3-hydroxybutyrate, *J. Mater. Sci.*, 1984, **19**, 2781-2794.

[3] N. Follain, C. Chappey, E. Dargent, F. Chivrac, R. Crétois and S. Marais, Structure and barrier properties of biodegradable polyhydroxyalkanoate films, *J. Phys. Chem. C*, 2014, **118**, 6165-6177.

[4] X. Wu, L. Pu, Y. Xu, J. Shi, X. Liu, Z. Zhong and S. Luo, Deformation of high density polyethylene by dynamic equal-channel-angular pressing, *RSC Adv.*, 2018, **8**, 22583-22591.

[5] R. Hielscher and H. Schaeben, A novel pole figure inversion method: specification of the MTEX algorithm, *J. Appl. Crystallogr.*, 2008, **41**, 1024–1037.

[6] F. Bachmann, R. Hielscher and H. Schaeben, Texture analysis with MTEX - free and open source software toolbox, *Solid State Phenom.*, 2010, **160**, 63–68.

[7] S. R. Andersson, M. Hakkarainen, S. Inkinen, A. Sodergard and A. C. Albertsson, Customizing the hydrolytic degradation rate of stereocomplex PLA through different PDLA architectures, *Biomacromolecules*, 2012, **13**, 1212-1222.

[8] R. Yang, Y. Qin, C. Li, L. Dai and Z. L. Wang, Characteristics of output voltage and current of integrated nanogenerators, *Appl. Phys. Lett.*, 2009, **94**, 022905.

[9] E. J. Curry, T. T. Leb, R. Das, K. Ke, E. M. Santorella, D. Paul, M. T. Chorsi, K. T. M. Tran, J. Baroody, E. R. Borges, B. Ko, A. Golabchi, X. Xin, D. Rowe, L. Yue, J. Feng, M. D. Morales-Acosta, Q. Wu, I.-P. Chen, X. T. Cui, J. Pachter and T. D. Nguyen, Biodegradable nanofiber-based piezoelectric transducer, *Proc. Natl. Acad. Sci. USA*, 2020, **117**, 214-220.

[10] B. Y. Lee, J. Zhang, C. Zueger, W.-J. Chung, S. Y. Yoo, E. Wang, J. Meyer, R. Ramesh and S.-W. Lee, Virus-based piezoelectric energy generation, *Nat. Nanotechnol.*, 2012, **7**, 351-356.

[11] D.-M. Shin, H. J. Han, W.-G. Kim, E. Kim, C. Kim, S. W. Hong, H. K. Kim, J.-W. Oh and Y.-H. Hwang, Bioinspired piezoelectric nanogenerators based on vertically aligned phage nanopillars, *Energy Environ. Sci.*, 2015, **8**, 3198-3203.

[12] S. K. Ghosh and D. Mandal, Sustainable energy generation from piezoelectric biomaterial for noninvasive physiological signal monitoring, *ACS Sustainable Chem. Eng.*, 2017**, 5**, 8836-8843.

[13] S. K. Ghosh and D. Mandal, Bio-assembled, piezoelectric prawn shell made self-powered wearable sensor for non-invasive physiological signal monitoring, *Appl. Phys. Lett.*, 2017**, 110**, 123701.

[14] K. Kim, M. Ha, B. Choi, S. H. Joo, H. S. Kang, J. H. Park, B. Gu, C. Park, C. Park, J. Kim, S. K. Kwak, H. Ko, J. Jin and S. J. Kang, Biodegradable, electro-active chitin nanofiber films for flexible piezoelectric transducers, *Nano Energy***,** 2018**, 48**, 275-283.

[15] N. R. Alluri, N. P. M. J. Raj, G. Khandelwal, V. Vivekananthan and S.-J. Kim, Aloe vera: A tropical desert plant to harness the mechanical energy by triboelectric and piezoelectric approaches, *Nano Energy*, 2020, **73**, 104767.

[16] K. Jenkins, S. Kelly, V. Nguyen, Y. Wu and R. Yang, Piezoelectric diphenylalanine

peptide for greatly Improved flexible nanogenerators, *Nano Energy*, 2018, **51**, 317-323.
[17] G. Zhang, Q. Liao, M. Ma, F. Gao, Z. Zhang, Z. Kang and Y. Zhang, Uniformly assembled vanadium doped ZnO microflowers/bacterial cellulose hybrid paper for flexible piezoelectric nanogenerators and self-powered sensors, *Nano Energy*, 2018, **52**, 501-509.